# Rapid Report

# Caveolin-1 modulates the activity of the volume-regulated chloride channel

Dominique Trouet, Bernd Nilius, Axel Jacobs*, Claude Remacle*,
Guy Droogmans and Jan Eggermont

*Laboratorium voor Fysiologie, Katholieke Universiteit Leuven, Campus Gasthuisberg,
B-3000 Leuven and *Laboratoire de Biologie Cellulaire, Université Catholique de Louvain,
B-1348 Louvain-La-Neuve, Belgium*

1.  Caveolae are small invaginations of the plasma membrane that have recently been implicated in signal transduction. In the present study, we have investigated whether caveolins, the principal protein of caveolae, also modulate volume-regulated anion channels (VRACs).

2.  $I_{Cl,swell}$, the cell swelling-induced chloride current through VRACs, was studied in three caveolin-1-deficient cell lines: Caco-2, MCF-7 and T47D.

3.  Electrophysiological measurements showed that $I_{Cl,swell}$ was very small in these cells and that transient expression of caveolin-1 restored $I_{Cl,swell}$. The caveolin-1 effect was isoform specific: caveolin-1$\beta$ but not caveolin-1$\alpha$ upregulated VRACs. This correlated with a different subcellular distribution of caveolin-1$\alpha$ (perinuclear location) from caveolin-1$\beta$ (perinuclear and peripheral).

4.  To explain the modulation of $I_{Cl,swell}$ by caveolin-1 we propose that caveolin increases the availability of VRACs in the plasma membrane or, alternatively, that it plays a crucial role in the signal transduction cascade of VRACs.

Caveolae are $\Omega$-shaped invaginations of the plasma membrane with a diameter of 50–100 nm that are present in many different cell types (Anderson, 1998). Caveolae form discrete lipid microdomains within the plasma membrane due to the preferential packing of sphingolipids and cholesterol. The principal protein component of caveolae is caveolin, a 21–24 kDa membrane protein that inserts into the caveolar membrane via an intramembrane hairpin loop. Four different isoforms encoded by three genes have been described: caveolin-1$\alpha$, -1$\beta$, -2 and -3 (Parton, 1996). Caveolins form homo- and hetero-oligomeric complexes (Song *et al.* 1997) that bind to cholesterol and sphingolipids, which seems to be an important step in the formation of caveolae (Li *et al.* 1996). Heterologous expression of caveolin-1 in lymphocytes or CaCo-2 cells that lack both caveolin-1 and morphological caveolae induces the appearance of caveolae in the plasma membrane (Fra *et al.* 1995; Mirre *et al.* 1996; Vogel *et al.* 1998). It has recently emerged that caveolae form specialised membrane compartments involved in signal transduction with caveolin-1 forming a molecular scaffold onto which signalling proteins such as the endothelial NO synthase, the c-src protein tyrosine kinase or small GTPases such as Ras and Rho are assembled in their inactive configuration (Okamoto *et al.* 1998).

Volume-regulated anion channels (VRACs) are expressed in most mammalian cell types and are involved in several basic cell functions such as cell volume regulation and electrogenesis (Nilius *et al.* 1997). The biophysical and pharmacological properties of the swelling-activated chloride current through VRACs ($I_{Cl,swell}$), have been described extensively (Nilius *et al.* 1997; Okada, 1997). In contrast, the signal transduction cascade that controls the gating of VRACs is only partially elucidated. In endothelial cells, a decrease in intracellular ionic strength rather than an increase in cell volume seems to be the crucial trigger for activation of VRACs (Voets *et al.* 1999), which also requires one or more tyrosine phosphorylation steps (Voets *et al.* 1998). In addition, the Rho/Rho kinase pathway seems to exert a permissive effect on the VRAC signal transduction cascade in endothelial cells (Nilius *et al.* 1999). Finally, the hypothesis has been put forward that activation of VRACs requires a specific plasma membrane organisation including membrane invaginations (Okada, 1997).

The function of caveolae as signal transducing compartments as well as the proposed role of plasma membrane invaginations in the activation of VRACs prompted us to investigate whether caveolae and/or caveolin might affect

VRAC activity. We therefore studied $I_{Cl,swell}$ in caveolin-1-deficient cell lines before and after transient transfection with caveolin-1.

# METHODS

## Cells

Human colon cancer cells Caco-2 (ECACC 86010202) and human breast cancer cells MCF-7 (ECACC 86012803), T47D (ECACC 85102201) and calf pulmonary artery endothelial cells (CPAE; ATCC CCL 209) were used. Cells were transiently transfected with the bicistronic pCINeo/IRES-GFP vector (green fluorescent protein, GFP; see also Trouet *et al.* 1997), containing the canine caveolin-1 cDNA (EMBL acession number Z12161; Kurczchalia *et al.* 1992). Using the QuickChange protocol (Stratagene, La Jolla, USA), pCINeo/IRES-GFP/caveolin-1 was mutagenised to generate pCINeo/IRES-GFP/caveolin-1α (methionine 32 replaced by isoleucine) or pCINeo/IRES-GFP/caveolin-1β (start codon replaced by tryptophan codon).

MCF-7, T47D and Caco-2 cells were directly seeded on gelatine-coated coverslips at $5 \times 10^3$ cells per coverslip, 24 h prior to transfection. MCF-7 cells were then transfected using 6 μl Superfect (Qiagen, Hilden, Germany) and 1·5 μg plasmid DNA per coverslip. For T47D and Caco-2 cells, transfection was performed using 2·4 μl Enhancer, 6 μl Effectene (Qiagen, Hilden, Germany) and 0·3 μg plasmid DNA per coverslip. Cells were analysed on days 2 and 3 after transfection.

## Solutions

Extracellular solutions (Krebs, isotonic Cs⁺ solution (320 ± 5 mosmol kg⁻¹) and the 25% hypotonic Cs⁺ solution (240 ± 5 mosmol kg⁻¹)) were as described previously (Voets *et al.* 1998). For anion substitution, NaCl was fully replaced by NaI or sodium

gluconate. In a few experiments, a hypertonic solution (420 ± 5 mosmol kg⁻¹) was used, which had been prepared by adding 100 mM mannitol to the isotonic Cs⁺ solution. A standard pipette solution (290 mosmol kg⁻¹) was used (Voets *et al.* 1998). The concentration of free Ca²⁺ in this solution was buffered at 100 nM to prevent activation of Ca²⁺-activated Cl⁻ currents.

## Electrophysiological recordings

Transfected green fluorescent cells were visualised in a patch-clamp set-up as described previously (Trouet *et al.* 1997). Currents were monitored with an EPC-7 patch-clamp amplifier (List Electronic, Lambrecht/Pfalz, Germany). Patch electrodes had DC resistances between 2 and 5 MΩ. An Ag–AgCl wire was used as reference electrode. In Cl⁻ substitution experiments, a 0·2 M NaCl agar bridge was used. Whole-cell membrane currents were measured using ruptured patches. Currents were sampled at 1 ms intervals. The following voltage protocol was applied every 15 s from a holding potential of −25 mV: a step to −80 mV for 0·2 s, followed by a step to −100 mV for 0·1 s, and a 1·5 s linear voltage ramp to +100 mV. Experiments were performed at room temperature.

## Analysis

Electrophysiological data were acquired with pCLAMP 5.5 (Axon Instruments) and analysed with WinASCD (G. Droogmans) and Origin 5.0 (Microcal). Time courses of the whole cell current were obtained by taking the current at +50 or −100 mV. Current–voltage relations were obtained from the currents measured during the linear voltage ramp. Difference currents were calculated by subtracting the basal current under isotonic conditions from the maximal current during hypotonic stimulation. Relative ion permeabilities ($P_x/P_{Cl}$) were calculated from shifts in reversal potential induced by anion substitution using a modified Goldman–Hodgkin–Katz equation. Pooled data are given as median and interquartile range (IQR) from $n$ cells except when explicitly stated otherwise (in which case means ± S.E.M. are given). Since the caveolin-1-transfected cell populations displayed non-normal distributions, the non-parametric Mann–Whitney $U$ test was used to test significance. Differences were considered significant at the level of $P < 0.03$.

## Immunofluorescence

Caco-2 cells (grown at a density of $6 \times 10^3$ cells per coverslip) were transfected with caveolin-1, -1α or -1β using the bicistronic GFP-expression vector. Forty-eight hours after transfection, cells were fixed for 15 min in phosphate-buffered saline (PBS) containing 3·7% formalin, rinsed with PBS and permeabilised with 0·2% Triton X-100 for 4 min at room temperature. Cells were washed with PBS and blocked with 10% fetal calf serum in PBS for 1 h. They were then successively incubated with PBS containing (i) a 1:400 dilution of anti-caveolin-1 monoclonal antibody (C37120, Transduction Laboratories) and (ii) *R*-phycoerythrin (PE)-conjugated goat anti-mouse IgG (Sigma ImmunoChemicals), for 1 h each. Cells were washed with PBS between incubations. Slides were observed under a BioRad 1024 confocal fluorescence microscope using the following settings: excitation with a krypton–argon laser at 488 nm; emission filter for fluorescein isothiocyanate (FITC): 522 ± 16 nm; emission filter for PE: 580 ± 16 nm. Transfected cells were identified by GFP fluorescence using the FITC settings and analysed for caveolin-1 expression using the PE settings. Control experiments showed a small contamination of the PE signal with the GFP signal, which was corrected by subtraction. The specificity of the PE signal was checked in control experiments using non-transfected cells or in GFP-negative cells. Neither of these displayed PE signals above background.
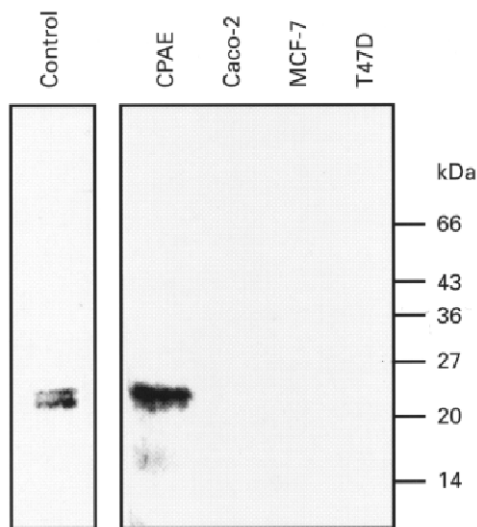


**Figure 1. Caveolin-1 is not expressed in Caco-2, MCF-7 and T47D cells**

Fifty micrograms of Caco-2, MCF-7 and T47D cell lysates were separated on SDS–PAGE (12·5% acrylamide), electroblotted and stained with a monoclonal antibody against caveolin-1. Human fibroblasts (left lane) and calf pulmonary artery endothelial cells (CPAE) were used as positive controls. The migration pattern of protein molecular mass standards (expressed in kDa) is shown on the right.

## Immunoblot analysis

CPAE, Caco-2, MCF-7 and T47D cells ($10^7$) were lysed in a hypotonic buffer (1 ml) containing 25 mM Tris-HCl pH 7·5, 20 mM NaCl, 2·5 mM EGTA, 0·5% (v/v) Nonidet P-40 and a protease-inhibitor cocktail (1 mM phenylmethylsulfonyl fluoride, 0·1 $\mu$g ml$^{-1}$ leupeptin). The lysate was centrifuged at 12 000 $g$ for 15 min and the supernatant stored at $-20$ °C. Fifty micrograms of protein was separated on SDS–PAGE (12·5% acrylamide) and transferred to a polyvinylidene difluoride (PVDF) microporous membrane (Immobilon, Millipore) by semi-dry electroblotting. Efficiency of blotting was checked by Ponceau S staining of the blots. Caveolin-1 was detected with a commercially available monoclonal antibody (C37120, Transduction Laboratories) diluted 1:1000. Secondary antibodies were alkaline phosphatase-conjugated goat anti-mouse IgG. Immunoreactive bands were visualised with the Vistra enhanced chemifluorescence detection kit (Amersham) on a Storm 840 imager (Molecular Dynamics).

# RESULTS

## Increase of $I_{Cl,swell}$ in caveolin-1-deficient cells by transient transfection with caveolin-1

Wild-type Caco-2 cells, which do not express caveolin-1 (Fig. 1 and see also Mirre *et al.* 1996), generate only a small membrane current when exposed to a 25% hypotonic stimulus (HTS) (Fig. 2*A*). The difference current (maximal HTS-induced current minus background current before HTS) was 1·73 pA pF$^{-1}$ (IQR 0·32–6·18 pA pF$^{-1}$; $n = 21$) at $+50$ mV. Swelling of Caco-2 cells during HTS was verified by visually inspecting cell volume on a video monitor. In contrast, a 25% HTS evoked a pronounced increase in membrane current in Caco-2 cells that were transiently transfected with caveolin-1 (Fig. 2*D*). In transfected cells, the difference current amounted to 22 pA pF$^{-1}$ (IQR 7·6–48 pA pF$^{-1}$; $n = 35$) at $+50$ mV. The following observations indicate that the HTS-induced current in Caco-2 cells transfected with caveolin-1 corresponds to the typical $I_{Cl,swell}$. (i) The current reversed around $-20$ mV, which is close to the predicted equilibrium potential for Cl$^-$ (Fig. 2*E*). (ii) Substituting extracellular Cl$^-$ with I$^-$ or gluconate resulted in, respectively, a leftward and rightward shift of the reversal potential indicating an I$^- >$ Cl$^- >$ gluconate permeability sequence (data not shown). The measured shifts in reversal potential were converted to permeability ratios resulting in $P_X/P_{Cl}$ ratios ($n = 8$) of 1·34 $\pm$ 0·02 for I$^-$ and 0·29 $\pm$ 0·03 for gluconate. (iii) The HTS-induced current displayed outward rectification (Fig. 2*E* and *F*). (iv) Inactivation was observed at positive potentials ($>40$ mV; Fig. 2*F*). Importantly, when Caco-2 cells were transfected with GFP alone, $I_{Cl,swell}$ amounted to



**Figure 2. Transfection of caveolin-1 in Caco-2 cells restores $I_{Cl,swell}$**

Membrane currents before, during and after 25% hypotonic stimulation (HTS) were recorded in a non-transfected Caco-2 cell (*A–C*) and in a Caco-2 cell transfected with caveolin-1 (*D–F*). *A* and *D*, time course of the current at $+50$ mV (upper trace) and at $-100$ mV (lower trace). During hypotonic stimulation (HTS), control cells developed only a small current with time (*A*), whereas in transfected cells a pronounced increase in membrane current is observed (*D*). The HTS-induced changes are reversible upon returning to isotonic conditions and completely disappear upon perfusion with a hypertonic solution (mann). *B* and *E*, *I–V* curves taken at the times marked by the filled symbols in *A* and *D*. The current–voltage relation of the membrane current at time zero in a typical control cell (a) and in a transfected cell (e) is compared to the respective *I–V* curves recorded during the plateau phase of the HTS-activated membrane current in the same control cell (b) and transfected cell (f). After switching back to isotonic conditions, the current returned to nearly control level (c and g). After application of a hypertonic mannitol solution (mann) the current reached its basal level (d and h). *C* and *F*, current traces during voltage steps applied at the time indicated by the asterisk in *A* and *D*. Note the different current scales. Voltage protocol: holding potential at $-50$ mV, steps between $-100$ and $+100$ mV, increment $+20$ mV.
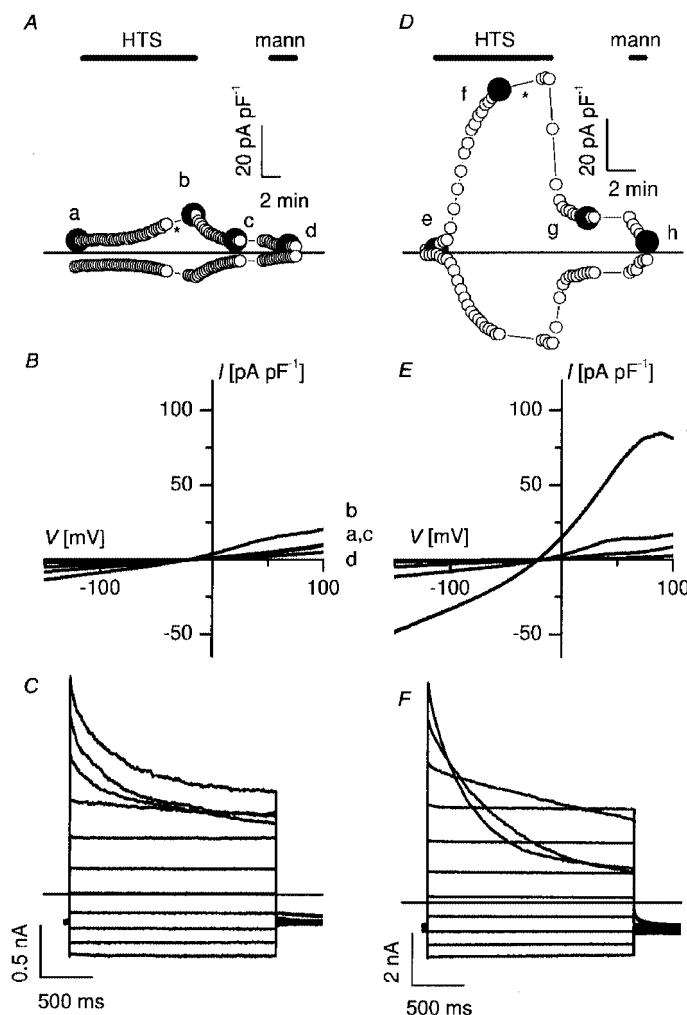
$86 \pm 15\%$ ($n = 6$) of $I_{Cl,swell}$ in control ($n = 17$) Caco-2 cells, thereby excluding the possibility that the above-described effects are caused by GFP. Previous observations in calf pulmonary endothelial (CPAE) cells had also shown that expression of GFP had no effect on the $I_{Cl,swell}$ amplitude (Vennekens et al. 1999). Capacitance of Caco-2 cells varied from 8 to 100 pF in control cells (median 40 pF; $n = 31$) and from 11 to 92 pF in GFP-transfected cells (median 28; $n = 35$).

We verified the effect of caveolin-1 on efficient activation of $I_{Cl,swell}$ in two other caveolin-1-deficient cell lines, MCF-7 and T47D (Fig. 1 and see also Lee et al. 1998). Wild-type MCF-7 and T47D displayed a small $I_{Cl,swell}$ after a 25% HTS. The HTS-induced difference current amounted to $5 \cdot 0$ pA pF$^{-1}$ (IQR $2 \cdot 0 – 8 \cdot 0$ pA pF$^{-1}$; $n = 7$) for MCF-7 and $6 \cdot 0$ pA pF$^{-1}$ (IQR $5 \cdot 0 – 9 \cdot 0$ pA pF$^{-1}$; $n = 11$) for T47D at +80 mV (Fig. 3). However, after transfection with caveolin-1, MCF-7 and T47D showed a marked activation of an outwardly rectifying chloride current by 25% HTS. In transfected cells, the HTS-induced difference current at +80 mV amounted to 12 pA pF$^{-1}$ (IQR 7–58 pA pF$^{-1}$; $n = 15$) in MCF-7 and 20 pA pF$^{-1}$ (IQR $7 \cdot 8 – 28$ pA pF$^{-1}$; $n = 11$) in T47D (Fig. 3). These values were significantly different from the values recorded in control cells.

## Caveolin-1$\beta$, but not caveolin-1$\alpha$, mediates the activation of VRACs

The caveolin-1 mRNA contains two translation initiation codons, one at position 1 and another at position 32 of the open reading frame. Translation initiation at codon 1 generates caveolin-1$\alpha$ (178 amino acids) whereas initiation at the distal AUG codon yields caveolin-1$\beta$, an NH$_2$-terminally truncated protein of 147 amino acids (Scherer et al. 1995). We mutated the AUG codons in the caveolin open reading frame either at position 32 (M32I) or at position 1 (M1W) to generate expression vectors for respectively caveolin-1$\alpha$ or caveolin-1$\beta$. Surprisingly, Caco-2 cells transfected with caveolin-1$\alpha$ showed no activation of VRACs during a 25% hypotonic stimulation ($n = 14$) (Fig. 3). In contrast, expression of caveolin-1$\beta$ in Caco-2 cells resulted in a significant activation of the hypotonicity-induced current with a median increase in current amplitude at +50 mV of $20 \cdot 35$ pA pF$^{-1}$ (IQR $9 \cdot 8 – 38 \cdot 6$ pA pF$^{-1}$; $n = 14$) (Fig. 3). The HTS-induced currents observed in caveolin-1- or caveolin-1$\beta$-transfected cells were phenotypically identical (data not shown).

## Confocal microscopy of caveolin-1-transfected Caco-2 cells

To find out whether the different effects of caveolin-1 isoforms on VRACs could be ascribed to differences in expression we performed confocal immunofluorescence microscopy on Caco-2 cells transiently transfected with caveolin-1, -1$\alpha$ or -1$\beta$ (Fig. 4). Confocal images of transfected cells confirmed the expression of caveolin-1, -1$\alpha$ or -1$\beta$. Thus the negative effect observed with caveolin-1$\alpha$ is not due to a deficient expression. Interestingly, in Caco-2 cells transfected with caveolin-1 or caveolin-1$\beta$ the fluorescent caveolin-1 signals were observed both in the perinuclear region and at the periphery of the cell. In contrast, in Caco-2 cells transfected with caveolin-1$\alpha$, the distribution pattern of the fluorescence signal was mainly perinuclear with no or very weak signals at the edge of the cell. This is consistent with a previous observation on
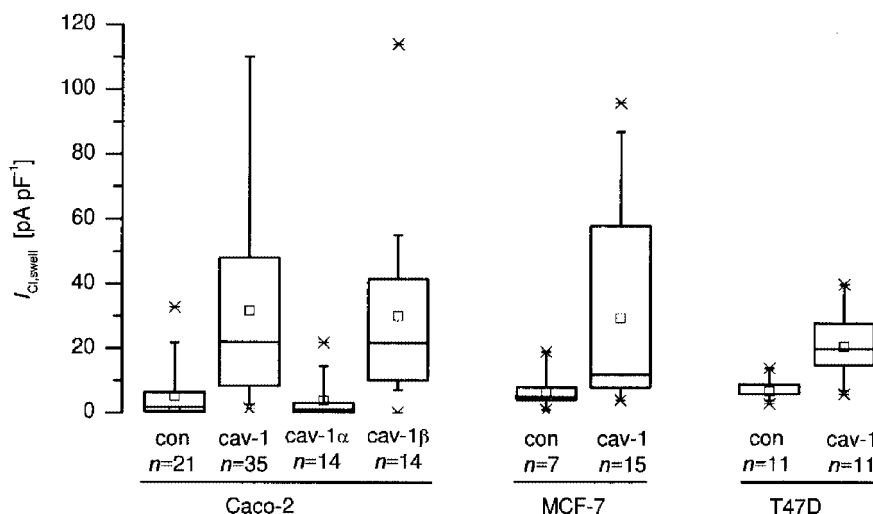


**Figure 3. Effect of caveolin-1 isoforms on $I_{Cl,swell}$ in caveolin-1-deficient cell lines**

Caco-2, MCF-7 and T47D cells, either control (con) or transfected with caveolin-1, -1$\alpha$ or -1$\beta$ as indicated, were subjected to a 25% HTS and $I_{Cl,swell}$ was measured. Difference currents (maximal HTS-triggered current minus basal current in isotonic medium) are plotted for the different conditions either at +50 mV (Caco-2) or at +80 mV (MCF-7 and T47D). The boxes correspond to interquartile ranges (25–75 percentile; middle line is median) with error bars representing the 5th (lower) and 95th percentile (upper). Small open square denotes the mean. Asterisks above and below boxes represent the 0th and 100th percentile. The differences between transfected and control conditions were statistically significant.
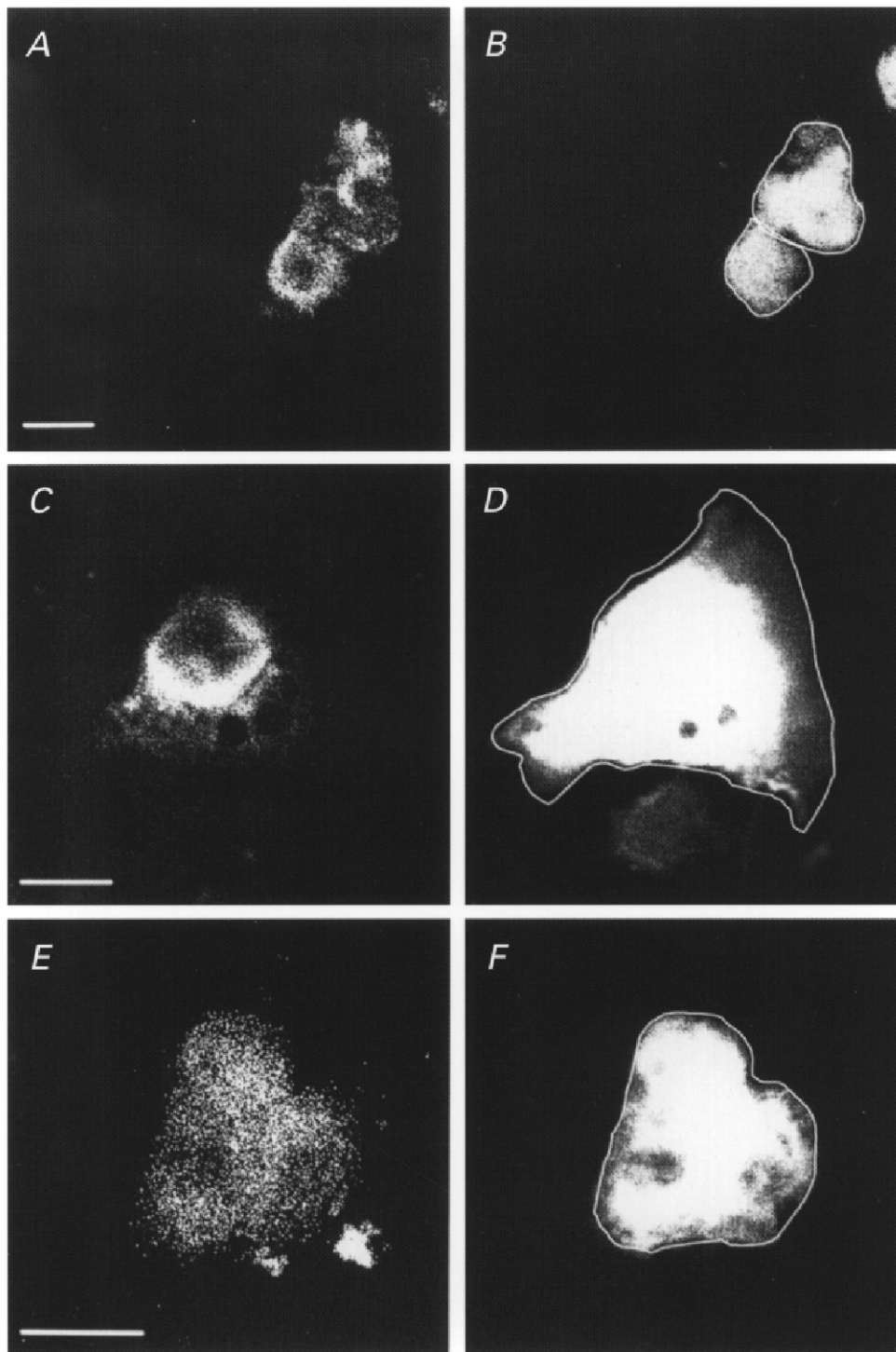
**Figure 4. Immunofluorescence of Caco-2 cells transfected with caveolin-1 isoforms**

Caco-2 cells were transfected with the bicistronic GFP expression vector containing caveolin-1 (*A* and *B*), -1$\alpha$ (*C* and *D*) or -1$\beta$ (*E* and *F*). The GFP fluorescent signal (*B*, *D* and *F*) was used to identify transfected cells and to define the cell border (white superimposed line in GFP panels). Caveolin-1 isoforms were visualised using a non-discriminating monoclonal antibody (*A*, *C* and *E*) and phycoerythrin-conjugated secondary antibodies. Images representative for the different conditions indicate that caveolin-1, -1$\alpha$ and -1$\beta$ are expressed. In addition, the subcellular distribution of caveolin-1$\alpha$ seems to be restricted to the perinuclear region, whereas the caveolin-1 and caveolin-1$\beta$ signals reach the cell periphery. Scale bar corresponds to 10 $\mu$m in all panels.

caveolin-1 distribution in transfected FRT cells where caveolin-1$\alpha$ preferentially accumulated in intracellular perinuclear membranes and caveolin-1$\beta$ was predominantly situated at the cell periphery (Scherer *et al.* 1995). Since the VRAC is a channel located in the plasma membrane, it is plausible that only plasma membrane-associated caveolin-1 contributes to the modulation of VRACs.

## DISCUSSION

In this study, we demonstrate for the first time that caveolin-1 contributes to the activity of VRACs. Indeed, we show for three different caveolin-1-deficient cell lines that a 25 % hypotonic stimulation induces either no or only a small $I_{Cl,swell}$ and that transient expression of caveolin-1 restores the $I_{Cl,swell}$ response. These observations are consistent with a previous finding in caveolin-1-deficient FRT cells where hypotonic stimuli induced only small currents with a long delay (Nilius *et al.* 1996). One possible explanation for this observation could be that caveolin-1-deficient cells do not swell if exposed to extracellular hypotonicity. However, the experimental conditions are nearly identical to those used by Voets *et al.* (1999) who showed a progressive increase in CPAE cell volume during superfusion with an extracellular hypotonic solution. Indeed, visual inspection of control Caco-2 cells revealed cell swelling during HTS application. Also, Altenberg *et al.* (1994) reported previously that MCF-7 cells swell when exposed to a hypotonic stimulus. An alternative, but rather implausible, explanation would be that caveolin-1 forms the VRAC channel itself. However, the proposed membrane topology for caveolin-1 is not compatible with it being a transmembrane ion channel. Indeed, membrane insertion of caveolin-1 is thought to occur via a hydrophobic hairpin which plugs into the cytosolic leaflet of the membrane but which does not traverse the entire lipid bilayer (for a review, see Parton, 1996). This leaves us with two possible explanations. (i) Caveolin-1 promotes $I_{Cl,swell}$ by increasing the availability of VRAC proteins in the plasma membrane, e.g. by facilitating or controlling its plasma membrane delivery. This possibility is consistent with the observation that caveolin-1 is involved in protein sorting to the apical membrane in polarised MDCK cells (Scheiffele *et al.* 1998). (ii) Caveolin-1 plays a role in the signal transduction cascade that converts cell swelling into channel activation. The documented role of caveolin-1 in signal transduction (see Introduction) is compatible with this mechanism. Unfortunately, the present ignorance and uncertainty about the molecular identity of the VRAC (for a review, see Nilius *et al.* 1997) precludes an experimental approach to discriminate unambiguously between these two alternatives.

With respect to the possible physiological significance of the VRAC–caveolin interaction, it is interesting to extrapolate our data to the physiology of endothelial cells. Being at the interface between blood and vessel wall, endothelial cells convert chemical and mechanical stimuli into the release of vasoactive substances such as NO. Several observations point to a crucial role for caveolae and/or caveolins in endothelial

signal transduction. (i) The conversion of mechanical stimuli into tyrosine phosphorylation signals appears to depend on intact caveolae (Rizzo *et al.* 1998). (ii) ATP-triggered intracellular $Ca^{2+}$ waves originate at specific caveolin-enriched cell edges (Isshiki *et al.* 1998). (iii) Caveolin-1 specifically regulates NO synthase activity by sequestering it in an inactive configuration to caveolae (Michel *et al.* 1997). (iv) It has previously been shown that mechanical stimulation of endothelial cells activates a $Cl^-$ channel that is very similar or identical to the VRAC (Nakao *et al.* 1999). We now demonstrate that VRAC activity can be modulated by caveolin. Thus, an overall picture is emerging whereby caveolae function as endothelial mechano- and chemotransducers. However, whether the observed caveolin–VRAC interaction is part of such a physiological transduction cascade remains to be shown.

In conclusion, we have identified a functional interaction between caveolin-1 and the VRAC which seems to be of crucial importance for efficient activation of VRACs by cell swelling. Thus, multiple factors such as ionic strength, protein phosphorylation, Rho/Rho kinase and caveolin-1 contribute to the activation and/or modulation of VRACs.

ALTENBERG, G. A., DEITMER, J. W., GLASS, D. C. & REUSS, L. (1994). P-glycoprotein-associated $Cl^-$ currents are activated by cell swelling but do not contribute to cell volume regulation. *Cancer Research* **54**, 618–622.

ANDERSON, R. G. W. (1998). The caveolae membrane system. *Annual Review of Biochemistry* **67**, 199–225.

FRA, A. M., WILLIAMSON, E., SIMONS, K. & PARTON, R. G. (1995). De novo formation of caveolae in lymphocytes by expression of VIP21-caveolin. *Proceedings of the National Academy of Sciences of the USA* **92**, 8655–8659.

ISSHIKI, M., ANDO, J., KORENAGA, R., KOGO, H., FUJIMOTO, T., FUJITA, T. & KAMIYA, A. (1998). Endothelial $Ca^{2+}$ waves preferentially originate at specific loci in caveolin-rich cell edges. *Proceedings of the National Academy of Sciences of the USA* **95**, 5009–5014.

KURZCHALIA, T. V., DUPREE, P., PARTON, R. G., KELLNER, R., VIRTA, H., LEHNERT, M. & SIMONS, K. (1992). VIP21, a 21-kD membrane protein is an integral component of trans-Golgi-network-derived transport vesicles. *Journal of Cell Biology* **118**, 1003–1014.

LEE, S. W., REIMER, C. L., OH, P., CAMPBELL, D. B. & SCHNITZER, J. E. (1998). Tumor cell growth inhibition by caveolin re-expression in human breast cancer cells. *Oncogene* **16**, 1391–1397.

LI, S., SONG, K. S., KOH, S. S., KIKUCHI, A. & LISANTI, M. P. (1996). Baculovirus-based expression of mammalian caveolin in Sf21 insect cells. A model system for the biochemical and morphological study of caveolae biogenesis. *Journal of Biological Chemistry* **271**, 28647–28654.

MICHEL, J. B., FERON, O., SACKS, D. & MICHEL, T. (1997). Reciprocal regulation of endothelial nitric-oxide synthase by $Ca^{2+}$-calmodulin and caveolin. *Journal of Biological Chemistry* **272**, 15583–15586.

MIRRE, C., MONLAUZEUR, L., GARCIA, M., DELGROSSI, M. H. & LE BIVIC, A. (1996). Detergent-resistant membrane microdomains from Caco-2 cells do not contain caveolin. *American Journal of Physiology* **271**, C887–894.

NAKAO, M., ONO, K., FUJISAWA, S. & IIJIMA, T. (1999). Mechanical stress-induced Ca$^{2+}$ entry and Cl$^-$ current in cultured human aortic endothelial cells. *American Journal of Physiology* **276**, C238–249.

NILIUS, B., EGGERMONT, J., VOETS, T., BUYSE, G., MANOLOPOULOS, V. & DROOGMANS, G. (1997). Properties of volume-regulated anion channels in mammalian cells. *Progress in Biophysics and Molecular Biology* **68**, 69–119.

NILIUS, B., GERKE, V., PRENEN, J., SZUCS, G., HEINKE, S., WEBER, K. & DROOGMANS, G. (1996). Annexin II modulates volume-activated chloride currents in vascular endothelial cells. *Journal of Biological Chemistry* **271**, 30631–30636.

NILIUS, B., VOETS, T., PRENEN, J., BARTH, H., AKTORIES, A., KAIBUCHI, K., DROOGMANS, G. & EGGERMONT, J. (1999). Role of Rho and Rho kinase in the activation of volume-regulated anion channels in bovine endothelial cells. *Journal of Physiology* **516**, 67–74.

OKADA, Y. (1997). Volume expansion-sensing outward-rectifier Cl$^-$ channel: fresh start to the molecular identity and volume sensor. *American Journal of Physiology* **273**, C755–789.

OKAMOTO, T., SCHLEGEL, A., SCHERER, P. E. & LISANTI, M. P. (1998). Caveolins, a family of scaffolding proteins for organizing "preassembled signaling complexes" at the plasma membrane. *Journal of Biological Chemistry* **273**, 5419–5422.

PARTON, R. G. (1996). Caveolae and caveolins. *Current Opinion in Cell Biology* **8**, 542–548.

RIZZO, V., SUNG, A., OH, P. & SCHNITZER, J. E. (1998). Rapid mechanotransduction in situ at the luminal cell surface of vascular endothelium and its caveolae. *Journal of Biological Chemistry* **273**, 26323–26329.

SCHEIFFELE, P., VERKADE, P., FRA, A. M., VIRTA, H., SIMONS, K. & IKONEN, E. (1998). Caveolin-1 and -2 in the exocytic pathway of MDCK cells. *Journal of Cell Biology* **140**, 795–806.

SCHERER, P. E., TANG, Z., CHUN, M., SARGIACOMO, M., LODISH, H. F. & LISANTI, M. P. (1995). Caveolin isoforms differ in their N-terminal protein sequence and subcellular distribution. Identification and epitope mapping of an isoform-specific monoclonal antibody probe. *Journal of Biological Chemistry* **270**, 16395–16401.

SONG, K. S., TANG, Z., LI, S. & LISANTI, M. P. (1997). Mutational analysis of the properties of caveolin-1. A novel role for the C-terminal domain in mediating homo-typic caveolin-caveolin interactions. *Journal of Biological Chemistry* **272**, 4398–4403.

TROUET, D., NILIUS, B., VOETS, T., DROOGMANS, G. & EGGERMONT, J. (1997). Use of a bicistronic GFP-expression vector to characterise ion channels after transfection in mammalian cells. *Pflügers Archiv* **434**, 632–638.

VENNEKENS, R., TROUET, D., VANKEERBERGHEN, A., VOETS, T., CUPPENS, H., EGGERMONT, J., CASSIMAN, J.-J., DROOGMANS, G. & NILIUS, B. (1999). Inhibition of volume-regulated anion channels by expression of the cystic fibrosis transmembrane conductance regulator. *Journal of Physiology* **515**, 75–85.

VOETS, T., DROOGMANS, G., RASKIN, G., EGGERMONT, J. & NILIUS, B. (1999). Reduced intracellular ionic strength as the initial trigger for activation of endothelial volume-regulated anion channels. *Proceedings of the National Academy of Sciences of the USA* **96**, 5298–5303.

VOETS, T., MANOLOPOULOS, V., EGGERMONT, J., ELLORY, C., DROOGMANS, G. & NILIUS, B. (1998). Regulation of a swelling-activated chloride current in bovine endothelium by protein tyrosine phosphorylation and G proteins. *Journal of Physiology* **506**, 341–352.

VOGEL, U., SANDVIG, K. & VAN DEURS, B. (1998). Expression of caveolin-1 and polarized formation of invaginated caveolae in Caco-2 and MDCK II cells. *Journal of Cell Science* **111**, 825–832.

## Corresponding author

J. Eggermont: Laboratorium voor Fysiologie, K. U. Leuven, Campus Gasthuisberg O&N, Herestraat 49, B-3000 Leuven, Belgium.

Email: jan.eggermont@med.kuleuven.ac.be